



**Universiteit
Leiden**
The Netherlands

Innovative (electro-driven) sample preparation tools for metabolomics study of muscle aging

He, Y.

Citation

He, Y. (2023, January 11). *Innovative (electro-driven) sample preparation tools for metabolomics study of muscle aging*. Retrieved from <https://hdl.handle.net/1887/3505583>

Version: Publisher's Version

License: [Licence agreement concerning inclusion of doctoral thesis in the Institutional Repository of the University of Leiden](#)

Downloaded from: <https://hdl.handle.net/1887/3505583>

Note: To cite this publication please use the final published version (if applicable).

Chapter 5

A sample preparation method for simultaneous profiling of signaling lipids and polar metabolites in small quantities of muscle tissues from a mouse model for sarcopenia

Based on:

Yupeng He, Marlien van Mever, Wei Yang, Luojiao Huang, Rawi Ramautar, Yvonne Rijksen, Wilbert P. Vermeij, Jan H.J. Hoeijmakers, Amy Harms, Peter Lindenburg, Thomas Hankemeier

A sample preparation method for simultaneous profiling of signaling lipids and polar metabolites in small quantities of muscle tissues from a mouse model for sarcopenia.

Metabolites (2022)

Abstract

The metabolic profiling of a wide range of chemical classes relevant to understanding sarcopenia under conditions in which sample availability is limited *e.g.* from mouse models, small muscles or muscle biopsies is desired. Several existing metabolomics platforms which include diverse classes of signaling lipids, energy metabolites, amino acids and amines would be informative for suspected biochemical pathways involved in sarcopenia. The sample limitation requires an optimized sample preparation method with minimal losses during isolation and handling and maximal accuracy and reproducibility. Here two developed liquid-liquid extraction sample-preparation methods, BuOH-MTBE-Water (BMW) and BuOH-MTBE-More-Water (BMMW), were evaluated and compared with previously reported methods, Bligh-Dyer (BD) and BuOH-MTBE-Citrate (BMC) for their suitability for these classes. The most optimal extraction was found to be the BMMW method, with the highest extraction recovery of 63% for the signaling lipids and 81% for polar metabolites, and acceptable matrix effect (close to 1.0) for all the metabolites of interest. The BMMW method was applied on muscle tissues as small as 5 mg (dry weight) from the well-characterized, prematurely aging, DNA repair-deficient *Ercc1^{Δ/-}* mouse mutant exhibiting multi-morbidity including sarcopenia. We successfully detected 109 lipids and 62 polar targeted metabolites. We further investigated whether fast muscle tissue isolation is necessary for mouse sarcopenia studies. A muscle isolation procedure involving 15 min at room temperature revealed a subset of metabolites to be unstable; hence, fast sample isolation is critical, especially for more oxidative muscles. Therefore, BMMW and fast muscle tissue isolation are recommended for future sarcopenia studies. This research provides a sensitive sample preparation method for simultaneous extraction of non-polar and polar metabolites from limited amounts of muscle tissue, supplies a stable mouse muscle tissue collection method, and methodologically supports future metabolomic mechanistic studies of sarcopenia.

1. Introduction

Sarcopenia is characterized by the age-related loss of muscle mass and function, and constitutes a major health problem, associated with a high loss of quality of life [1, 2]. Globally, 11–50% of those aged 80 or above suffer from sarcopenia [3], and this number is increasing with the rapid growth of the ageing population, thereby creating an enormous socio-economic and health care burden. The molecular mechanisms underlying sarcopenia are still not well understood and effective medication is lacking [4]. Metabolomics is a powerful approach for obtaining molecular insight into complex diseases and for discovery of disease biomarkers [5]. Previous muscle function metabolomics studies revealed that dysregulation of signaling lipids (*i.e.*, oxylipins, free fatty acids, oxidative stress markers) [6-8], energy metabolites (*i.e.*, ATP, citrate, pyruvate) [9-11], amino acids and amines [10, 12, 13] were highly associated with weak muscle contractile function. Therefore, a systematic metabolomics mechanistic study of these non-polar (signaling lipids) and polar (energy metabolites, amino acids, and amines) metabolites is needed for understanding the biochemistry behind sarcopenia and for the identification of biomarkers for diagnosis, prevention, and treatment of sarcopenia. Mice deficient in the DNA excision-repair gene *Ercc1* (*Ercc1^{Δ/-}*) show numerous age-related pathologies and accelerated ageing features [14-16], and are widely used in the studies of ageing and age-related diseases, including muscle wasting and sarcopenia [17-20]. Moreover, this mouse mutant is an excellent model for several rare, but very severe progeroid human DNA repair syndromes, including Cockayne syndrome, xeroderma pigmentosum, Fanconi anemia and XFE1 syndrome [21-23]. As the *Ercc1^{Δ/-}* mice exhibit early cessation of growth, only small amounts (*i.e.*, 5-50 mg dry weight) of (skeletal) muscle can be collected, necessitating development of a single sensitive, reproducible sample preparation method suitable for analysis by multiple metabolomics platforms, allowing analysis of non-polar and polar metabolites.

The Bligh and Dyer (BD) method is a traditional sample preparation method for the extraction of non-polar and polar components, able to non-selectively extract a wide range of metabolites [24, 25]. Medina *et al.* evaluated sample extraction methods with isopropanol and 1-butanol:methanol for simultaneous extraction of 584 non-polar and 116 polar metabolites, however, the method mainly focused on metabolome analysis of human plasma samples, and some of our targeted signaling lipids, *i.e.*, oxylipins, bile acids, were not covered [26]. Löfgren *et al.* developed an automated butanol:methanol extraction method

for lipids, however, the method mainly focused on the plasma lipid classes, *i.e.*, cholesterol, triacylglycerol, phosphatidylcholine, sphingomyelin, and lyso-phospholipids [27]. BuOH-MTBE-Citrate (BMC) is a sensitive sample preparation method for sample limited applications: Di Zazzo *et al.* applied for analysis of oxylipins, oxidative stress markers, endocannabinoids, and bile acids for ocular surface cicatrizing conjunctivitis, and identified 9S-hydroxy octadecatrienoic acid (9S-HOTrE) and 5-hydroxy eicosapentaenoic acid (5-HEPE) as potential diagnostic biomarker candidates. However, the performance of BMC on small amount of muscle tissues still remains unknown, and because of the addition of a non-volatile (citric acid/phosphate) buffer, the extracted aqueous phase was not compatible with mass spectrometric detection [28].

In this work, we report the development of a sample preparation method allowing the simultaneous extraction of targeted non-polar and polar metabolites from biomass-limited mouse muscle tissues (*i.e.*, 5-50 mg dry weight). With this approach, we would like to obtain more insight into the etiology of sarcopenia using a metabolomics approach. For this purpose, two extraction methods based on BMC [28] were developed and compared with Di Zazzo *et al.*'s BMC [28] and BD methods [29]. The optimal method with the highest extraction recovery and acceptable matrix effect was applied to muscle tissues of *Ercc1^{Δ/Δ}* mice to study the effect of the muscle tissue isolation speed on metabolite stability. Overall, this work yielded a sensitive sample preparation method for simultaneous extraction of non-polar and polar metabolites from limited amounts of muscle tissues, supplied a reference method for an existing sarcopenia samples collection, and methodologically supports the metabolomic analysis of sarcopenia.

2. Materials and Methods

2.1 Chemicals

Methanol and chloroform were purchased from Biosolve Chimime SARL (Dieuze, France). 1-butanol was purchased from Acros Organics (Geel, Belgium). Butylated hydroxytoluene (BHT) and methyl tertbutyl ether (MTBE), citric acid and sodium dihydrogen phosphate dehydrate were obtained from Sigma-Aldrich (Steinheim, Germany). MilliQ water was obtained from a Millipore high purity water dispenser (Billerica, MA, USA). All solvents were HPLC grade or higher.

For internal standards (ISTDs), deuterium-, carbon- and/or nitrogen-labelled metabolites were used. Labelled oxylipins, fatty acids, and endocannabinoids ISTDs were acquired from Cayman Chemicals (Ann Arbor, MI, USA). Labelled lysophospholipids, sphingolipids, bile acids and steroid ISTDs were ordered from Avanti Polar Lipids (Alabaster, AL, USA). Labelled amino acids and amine ISTDs were ordered from Cambridge Isotope Laboratories (Andover, MA, USA), labelled ATP, AMP and UTP were purchased from Sigma-Aldrich (Steinheim, Germany).

2.2 ISTDs preparation

For lipid ISTDs, the stock solution was prepared in MeOH in a stated concentration (Table S1) containing 0.4 mg/mL BHT. This includes the classes of oxylipins, fatty acids, endocannabinoids, bile acids and steroids, lysophospholipids and sphingolipids. For the stock solution of amino acids and amine ISTDs, 9 kinds of ISTDs (Table S2) were prepared in MilliQ water with the concentration of 0.5 mg/mL. Stock solutions of ATP ($^{13}\text{C}_{10}, ^{15}\text{N}_5$), AMP ($^{13}\text{C}_{10}, ^{15}\text{N}_5$), and UTP ($^{13}\text{C}_9, ^{15}\text{N}_2$) were prepared in MilliQ water at 10mg/mL (Table S3).

2.3 Muscle samples

The development and evaluation of extraction methods were performed on pig muscle tissues serving as a uniform source for multiple experiments and as a surrogate for mouse tissue which was only available in scarce quantities. The pig muscle tissue was stored at -80 °C before extraction. Muscle tissue from mice deficient in the DNA excision-repair gene *Ercc1* (*Ercc1 Δ ⁻*) was utilized for the study of effect of sample isolation speed on metabolite stability for sarcopenia. The generation and characterization of *Ercc1 Δ ⁻* mice is described in [15, 16, 20]. Three kinds of muscle types, gastrocnemius + soleus (Gas + Sol), quadriceps (Quadr), and extensor digitorum longus + tibialis anterior (EDL + TA) were collected at the animal facility of the Erasmus Medical Center, Rotterdam, Netherlands. All above experiments were performed in accordance with the Principles of Laboratory Animal Care and with the guidelines approved by the Dutch Ethical Committee (permit no. 139-12-13, and 139-12-18) in full accordance with European legislation.

Fast and delayed (15 min delayed) muscle tissue collection procedures were applied to study the effects of sample isolation speed on metabolite stability. Briefly, mice were anaesthetized using CO₂. For fast sample isolation, a large piece of Quadr tissue was

dissected immediately and rapidly frozen in liquid nitrogen, EDL + TA and Gas + Sol tissue were carefully isolated as described in [30]. Following dissection, the muscles were immediately frozen in liquid nitrogen-cooled isopentane and stored at -80 °C [19]. For delayed sample isolation, the Quadr, EDL + TA and Gas + Sol tissues from the other hind leg of the same mouse were kept 15 min at room temperature, then were isolated and frozen as described above for the fast isolation. All samples were stored at -80 °C until analysis.

2.4 Extraction methods

For the development of an extraction method yielding high extraction efficiency for both polar metabolites and signaling lipids, four extraction methods were compared and evaluated using pig muscle tissues, *i.e.*, the Bligh-Dyer (BD), BuOH-MTBE-Citrate (BMC), BuOH-MTBE-Water (BMW), and BuOH-MTBE-more-Water (BMMW) extraction. 30 mg ($\pm 20\%$) frozen wet pig muscle tissue was lyophilized in a VaCo I freeze-dryer (Zirbus, Bad Grund, Germany; connected to a E2M12 high vacuum pump, Edwards, Crawley, England) for 24 hours, and weighed. To homogenize muscle tissues thoroughly, a dry-homogenization method was used adding 100 mg ($\pm 10\%$) zirconium oxide beads (0.5 mm; Next Advance, Averill Park, NY, USA) to the freeze-dried tissue, and homogenized in a Bullet Blender (BBX24; Next Advance, Averill Park, NY, USA) for 15 min at speed 9 [29]. Labelled ISTDs (10 μ L amino acids & amines, 10 μ L ATP & AMP & UTP, 10 μ L lipids stock solution) were spiked in the muscle samples before and after extraction for the evaluation of the four extraction methods.

2.4.1 Bligh-Dyer extraction (BD)

A previously reported Bligh-Dyer extraction was utilized for the polar and non-polar analyte extraction [29]. Briefly, 400 μ L cold MeOH and 125 μ L cold MilliQ water were added to the muscle tissues and homogenized by using the Bullet Blender for 15 min at speed 9. Then 450 μ L homogenate was transferred to a new tube after centrifugation ($500 \times g$, 5 min, 4 °C), and vortexed with cold chloroform (450 μ L), water (250 μ L) and MeOH (50 μ L) for 2 min. The samples were next left on ice for 10 min to partition, and centrifuged ($2,000 \times g$, 10 min, 4 °C) to obtain a clear biphasic mixture. The 500 μ L upper aqueous/polar phase and 400 μ L lower organic/non-polar phase were collected separately by using positive-displacement Microman pipettes (Gilson, Middleton, WI, USA) without disturbing the layer between both phases. These were then evaporated in a SpeedVac Vacuum

concentrator (Thermo Savant SC210A, Waltham, Massachusetts, United States), and reconstituted in 50 μ L MeOH for the organic phase and 100 μ L 50% MeOH 50% MilliQ water for the aqueous phase.

2.4.2 *BuOH-MTBE-Citrate extraction (BMC)*

A reported lipid extraction method [28], BuOH-MTBE-Citrate extraction (BMC), was tested for the muscle samples. In this method, 5 μ L antioxidant solution (0.4 mg/mL BHT:EDTA=1:1), 150 μ L of 0.2M citric acid-0.4M disodium hydrogen phosphate buffer at pH 4.5, and 1 mL extraction solution (BuOH: MTBE=1:1, v/v) were added to all samples and allowed to settle on ice for 20 min before homogenization in the Bullet Blender for 15 min at speed 9. Then the homogenized samples were centrifuged (2,000 \times g, 4 $^{\circ}$ C) for 10 min, and 900 μ L of the upper organic phase was collected, evaporated, and reconstituted using the same method described in 2.4.1 BD method.

2.4.3 *BuOH-MTBE-Water extraction (BMW)*

The extraction procedure for the BMW method is similar to the BMC method but the 150 μ L citric acid/phosphate buffer was replaced with 150 μ L of cold MilliQ water. After collection of the upper organic phase, 500 μ L more ice-cold MilliQ water was added to more easily collect the lower aqueous phase. After vortexing and centrifugation at 2,000 \times g, 4 $^{\circ}$ C for 10 min, 350 μ L of the lower aqueous phase was then collected.

2.4.4 *BuOH-MTBE-More-Water extraction (BMMW)*

A larger aqueous phase volume (400 μ L of cold MilliQ water) was utilized in BMMW method instead of the 150 μ L of cold MilliQ water used in BMW method. 200 μ L of the lower aqueous phase was directly collected after collection of the upper organic phase.

2.5 **LC/CE-MS quality control**

Some extra extracted pig muscle tissues were pooled together as quality control (QC) samples. A QC sample was injected once each 6-8 samples to evaluate and correct for changes in sensitivity of the instruments. The metabolites with relative standard deviation (RSD) of quality control (QC) samples less than 30% were used for statistical analysis.

2.5.1 *Lipid metabolite analysis*

The signaling lipid metabolites were measured according to a validated ultra-performance liquid chromatography tandem mass spectrometry (UPLC-MS/MS) method in our lab [28].

Briefly, each sample was measured with two complementary reverse phase methods using mobile phases with different pH.

The low pH run utilized an Acquity BEH C18 column (50 × 2.1 mm, 1.7 μm; Waters, USA) on a Shimadzu LC-30AD (Japan) hyphenated to a SCIEX Q-Trap 6500+ (Framingham, MA, USA) Separations were performed using three mobile phases: (A) water with 0.1% acetic acid; (B) ACN: MeOH (9:1, v/v) with 0.1% acetic acid; (C) Isopropanol with 0.1% acetic acid at 40 °C at a flow rate of 0.7 mL/min. The 16 minute run used the following gradient: start with 20% B and 1% C; B was increased to 85% between 0.75 and 14 min, and C was increased to 15% between 11 and 14 min; the condition held for 0.5 min prior to column re-equilibration at the starting conditions from 14.8 to 16 min. Data was acquired using Sciex Analyst software (Version 1.7, Framingham, MA, USA) and peak integration used Sciex OS (Version 1.4.0, Framingham, MA, USA).

The high pH run used a Kinetex® Core-Shell EVO 100 Å C18 column (50 × 2.1 mm, 1.8 μm; Phenomenex, USA) on a Shimadzu LCMS-8060 system (Shimadzu, Japan) . Separations used mobile phases (A) 5% ACN with 2 mM ammonium acetate and 0.1% ammonium hydroxide and (B) 95% ACN with 2 mM ammonium acetate and 0.1% ammonium hydroxide at 40 °C at a flow rate of 0.6 mL/min. The gradient started with 1% B; B was increased to 100% from 0.7 to 7.7 min; 100% B held for 0.75 min prior to re-equilibration at the starting conditions between 8.75 and 11 min. Multiple reaction monitoring (MRM) was utilized in MS/MS acquisition in both positive and negative electrospray ionization mode with polarity switching. Data was acquired and peaks integrated using LabSolutions (Version 5.97 SP1, Shimadzu, Japan).

2.5.2 Energy metabolites analysis

The energy metabolites were analyzed using a hydrophilic interaction liquid chromatography (HILIC) mass spectrometry platform [31]. Briefly, a SeQuant ZIC-cHILIC column (PEEK 100 × 2.1 mm, 3.0 μm particle size; Merck KGaA, Darmstadt, Germany) was used on a Waters UPLC (Acquity™, Milford, MA, USA) coupled with a Sciex MS (Triple-TOF 5600+, Framingham, MA, USA). The separation method used mobile phases (A) 90% ACN with 5 mM ammonium acetate at pH 6.8; (B) 10% ACN with 5 mM ammonium acetate at pH 6.8, at a flow rate of 0.25 mL/min at 30 °C. The gradient method was: 100% A for 2 min; ramping 3–20 min to 60% A; ramping 20–20.1 to 100% A

and re-equilibrated to 35 min with 100% A. The MS data were acquired at full scan range 50–900 m/z in negative ionization mode at 400 °C by Sciex Analyst (Version 1.7, Framingham, MA, USA) and peaks were integrated using MultiQuant (Version 3.0.1, Sciex, Framingham, MA, USA).

2.5.3 Amino acids and amines analysis

The amino acids and amines were analyzed by a sheath-liquid Agilent 7100 capillary electrophoresis (CE) system, coupled to an Agilent mass spectrometer (TOF 6230, Waldbronn, Germany), and acquired by MassHunter Data Acquisition (Version B.05.01, Agilent, Santa Clara, California, USA). Fused-silica capillaries (BGB Analytik, Harderwijk, Netherlands) with a total length of 70 cm and an internal diameter of 50 μm were utilized. The CE separation voltage was 30 kV, and 10% acetic acid in water was used as background electrolyte (BGE) solution. The sheath-liquid, a mixture of water and isopropanol (50:50, v/v) containing 0.03% acetic acid, was delivered at a flow rate of 3 $\mu\text{L}/\text{min}$ by an Agilent 1260 Infinity Isocratic Pump (Waldbronn, Germany). The nebulizer gas was set to 0 kPa, the sheath gas flow rate was set at 11 L/min and the sheath gas temperature was set at 100 °C. The ESI capillary voltage was set at 5500 V. Fragmentor and skimmer voltages were 150 V and 50 V, respectively. MS data were acquired in positive ion mode between 50 and 1000 m/z with an acquisition rate of 1.5 spectra/s [32]. The amino acids and amines peaks were integrated using MassHunter Quantitative Analysis (Version.05.02, Agilent, Santa Clara, California, USA).

2.6 Data analysis

For metabolites stability evaluation in mouse muscle tissue, the response ratio was used and obtained by Equation 1:

$$\text{Response ratio} = \frac{\text{Peak area of the target metabolite}}{\text{Peak area of the assigned ISTD}} \quad (\text{Equation 1})$$

For metabolites for which QC samples had an RSD less than 30%, the response ratios were corrected by QC response ratio, and further normalized by the muscle tissue dry weight. For metabolites that can be measured by multiple platforms, *i.e.*, amino acids/amines (can be measured by HILIC and CE method in 2.5.2 and 2.5.3, respectively), some fatty acids (can be measured by both low- and high-pH lipid platforms), the results with smaller QC RSD was utilized (Table S4 and S5).

For the comparison and evaluation of the developed extraction methods, extraction recovery and matrix effect were utilized. Extraction recovery was calculated as the ratio of the ISTDs spiked at the start of the extraction procedure and the ISTDs spiked to the injection solvent prior to MS measurement. This value does not reflect the extraction recovery of metabolites from muscle tissue, but the loss of targeted metabolites during the liquid-liquid extraction process. Matrix effect was calculated by the ratio of ISTDs extracted from a muscle sample and a blank sample with only extraction solvents.

For selection of the optimal extraction method, the percentage of number of the highest extraction recovery for ISTDs for each extraction method was used and calculated by Equation 2:

$$\text{Percentage (\%)} = \frac{\text{The number of highest recovery in ISTDs}}{\text{The number of total ISTDs}} \times 100\% \quad (\text{Equation 2})$$

RStudio (Version 1.4.1106) and R (Version 4.0.5) was used for the data statistical analysis, all the figures were made by Graphpad Prism (Version 8.1.1, San Diego, California, USA).

3. Results and discussion

3.1 Development and evaluation of the sample preparation methods

Four sample preparation methods, *i.e.*, BD, BMC, BMW, BMMW, were systematically compared and evaluated with respect to extraction recovery and matrix effect for a range of metabolite classes by spiking carbon or deuterium labelled metabolites (ISTDs) using pig muscle tissue as a surrogate for mouse muscle during method development.

3.1.1 Extraction of signaling lipids

Five classes of lipid metabolites, *i.e.*, oxylipins, lysophospholipids & sphingolipids, free fatty acids, bile acids & steroids, and endocannabinoids, were analyzed in the organic phase for evaluation of the four extraction methods. Figure 1A showed that the extraction recovery of these lipids using BMC (orange), BMW (brown) and BMMW (yellow) were significantly higher than when using the BD (blue) method. This may be due to the utilization of the more non-polar solvents, MTBE and BuOH (relative polarity is 0.124 and 0.586, respectively [33]), for signaling lipids extraction in BMC, BMW and BMMW than the two less non-polar solvents, chloroform and MeOH (relative polarity is 0.259 and 0.762, respectively [33]), in BD. The higher non-polar property contributed to a higher partitioning of all signaling lipids in the organic phase in BMC, BMW and BMMW. Similar results

were also reported in [34], which indicated that lipids in hydrophobically associated form can more easily be extracted by relatively non-polar solvents, and the polar solvents, *i.e.*, ethanol and methanol, can disrupt the hydrogen bonding or electrostatic forces between membrane-associated lipids and protein.

Lower recovery values of lysophospholipids and sphingolipids (< 91%), and some bile acids, *i.e.*, GCA-d₄ (2%-71%) and DCA-d₄ (70%-83%), were observed in all four extraction methods compared to other lipid metabolites. The reason for the lower yield because of less non-polar properties of lysophospholipids & sphingolipids (logP=2.6-5.4), GCA (logP=1.4) and DCA (logP=3.3) than the other classes of lipid metabolites, *i.e.*, fatty acids (logP=6.0-6.8) endocannabinoids (logP=5.7-6.7), and oxylipins (logP=3.1-5.9). The higher recovery of oxylipins reported using the BD method (around 100%) in Alves *et al.*'s study compared with our BMMW method (>73%) results from the combination of both organic and aqueous phases for the measurement of these polar lipids [29]. Here, we compared just the organic phase extraction performance for lipid metabolites in the four sample preparation methods.

To determine the matrix effects of the four extraction methods on the targeted lipid measurements, signals of spiked internal standards in samples with and without muscle tissue were investigated. For most of the signaling lipids, matrix effect values (Figure 1B) ranged between 0.7-1.4, indicating that there is acceptable impact on MS measurements from muscle tissue matrix for all four extraction methods.

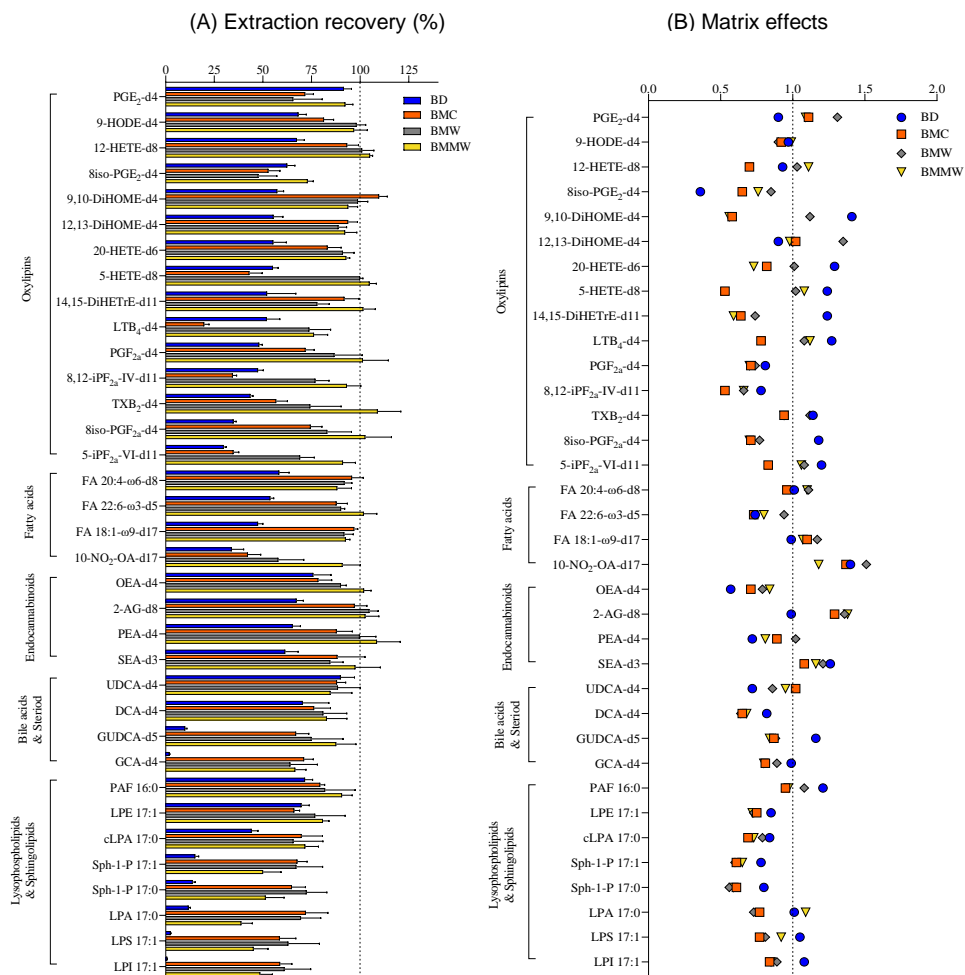


Figure 1. The extraction recovery (%) (A) and matrix effect (B) of lipids ISTDs by using the four extraction methods: BD, BMC, BMW, and BMMW.

3.1.2 Extraction of polar metabolites

As a nonvolatile (citric acid/phosphate) buffer was utilized in the published BMC method, the aqueous phase was rendered unsuitable for the intended LC-MS analysis methods. In addition, the exogenous citric acid affected the analysis of one of our target metabolites, citric acid. Therefore, the aqueous phase of BMC method was not considered for the polar metabolites analysis. Two separation methods for polar metabolites, *i.e.*, HILIC for central energy metabolites, and CE for amino acids & amines, were used to evaluate the extraction of polar metabolites into the aqueous phase for the three extraction methods (BD, BMW, BMMW). For amino acids and amines, the extraction recoveries in BMW (brown) and BMMW (yellow) were significantly higher than in BD (blue) (Figure 2A). For energy metabolites, the recovery of ATP and UTP in BMW and BMMW was notably better than in BD, however, the recovery of AMP was dramatically lower compared to BD (Figure 2A). This might be the result of one extra 2 min vortex step with chloroform, water and MeOH at room temperature in BD, which accelerated the hydrolysis of ATP (or ADP) to AMP. Similar results showing ATP hydrolysis at room temperature was also observed in Becker *et al.*'s study [35]. Bruno *et al.* preferred the BD method for polar metabolites in mouse muscle over MeOH/Water extraction method but did not evaluate other methods [36]. Because of stability issues, we concluded the BD method was not the optimal extraction method for the HILIC measurements of energy metabolites from muscle tissues for our study.

When evaluating the performance of the extraction methods for the CE measurements of amino acids and amines, we noted the relatively low recovery obtained for tryptophan (28%-50%). This may be due to its high susceptibility to oxidative degradation [37]. Additionally, its weak polar property ($\log P = -1.1$) and low water solubility (1.36 mg/mL) among this class of metabolites ($\log P$ ranges from -2.0 to -5.4, water solubility ranges from 80.6 to 210 mg/mL) may contribute to a lower distribution of tryptophan in the aqueous phase during the extraction process. The weak polar property of UTP ($\log P = -3.4$) may have also contributed to its lower distribution in the aqueous phase compared to ATP ($\log P = -5.1$). The lower extraction recovery of UTP than weakly polar amino acids and amines, *i.e.*, valine ($\log P = -2.0$), may be due to the much higher water solubility of valine (210 mg/mL) than UTP (8.37 mg/mL). Matrix effect values (Figure 2B) were close to 1 for most of the

polar metabolites, demonstrating small impacts from extraction methods and the muscle tissue matrix on MS measurement for the targeted polar metabolites.

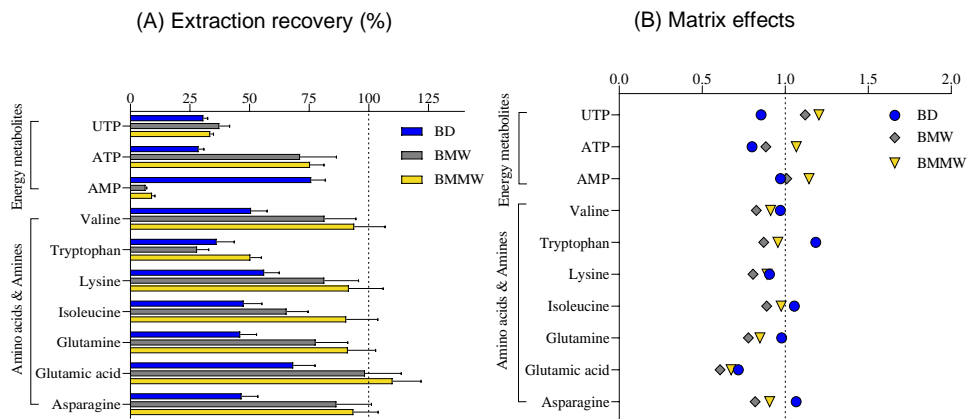


Figure 2. The extraction recovery (%) (A) and matrix effect (B) of polar ISTDs by using the extraction methods: BD, BMW, and BMMW.

3.1.3 Assessment of sample preparation method yielding optimal recovery for signaling lipids and polar metabolites

The performance of four extraction methods (BD, BMC, BMW, and BMMW) for signaling lipids, and three extraction methods (BD, BMW, and BMMW) for polar metabolites were evaluated and compared by calculating the percentage of the highest extraction recovery for each extraction method for different internal controls for each of the two chemical categories (Equation 2). The BMMW method turned out to give the best recovery as deduced from reaching the highest percentage of spiked internal standards for both non-polar (63%) and polar (81%) metabolites (Figure 3), demonstrating this method resulted in the smallest loss of metabolites during the sample preparation procedure in BMMW for all classes of metabolites of interest. BD was not preferred for mouse muscle extraction not only because of the lower recovery and percentage values, but also due to the rapid hydrolysis observed for ATP (or ADP) to AMP, and the labor required for the reproducible separation of organic and aqueous phase [24]. Therefore, BMMW was chosen as the extraction method of choice for the targeted non-polar and polar metabolites from small quantities of mouse muscles.

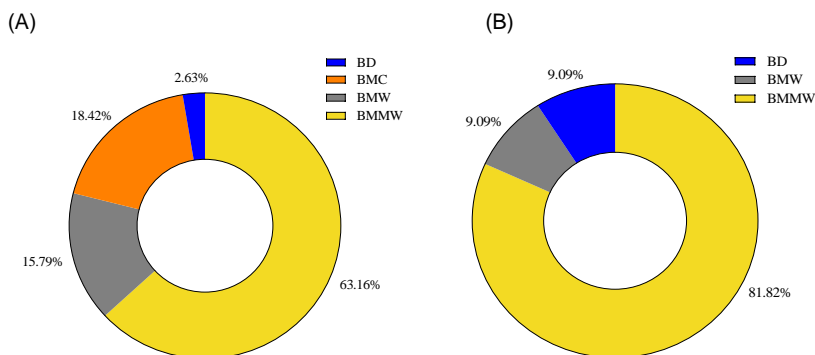


Figure 3. The percentage of the highest extraction recovery each method occupied in (A) signaling lipids and (B) polar metabolites.

3.2 Performance of the optimal sample preparation method in mouse muscle samples

For the metabolic profiling of mouse muscle, the reported LC-MS and CE-MS detection methods for lipid metabolites [38], energy metabolites [31], amino acids and amines [32] were utilized. 109 non-polar and 62 polar targeted metabolites were clearly observed (with a signal to noise ratio >10) using the LC-MS and CE-MS detection platforms to analyze *Ercc1^{Δ/-}* mouse muscle tissues (Figure 4). The detailed information of these non-polar (lipid) and polar metabolites for LC-MS and CE-MS analysis is provided in Table S4 and S5, respectively, in supporting information. As the sample collection procedure can also influence metabolite levels, the effect of muscle isolation speed on metabolite stability for these targeted metabolites was further investigated.

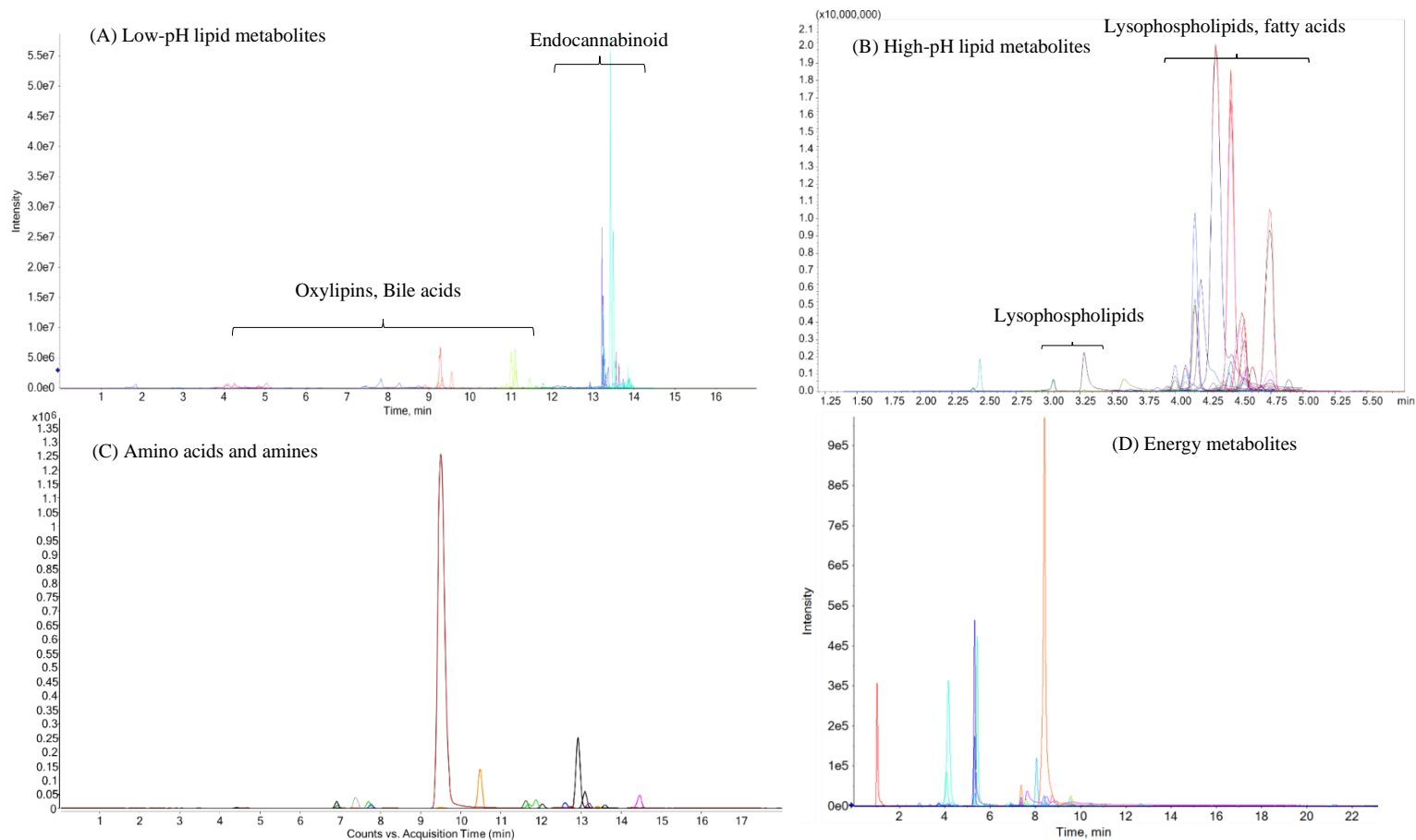


Figure 4. Representative LC(A, B and D)/CE (C)-MS chromatograms from different classes of metabolites obtained from *Ercc1* Δ - mouse muscle samples.

3.3 The effects of sample isolation speed on metabolite stability

To deduce the effect of sample collection speed on metabolites stability, the response ratios (Equation 1) of metabolites in fast and delayed muscle tissue isolation were investigated in three muscle specimens, namely the lower hindlimb muscles gastrocnemius and soleus (Gas + Sol), the extensor digitorum longus + tibialis anterior (EDL + TA), and the upper hindlimb muscle quadriceps (Quadr), which are the most commonly used mouse muscles for molecular analyses. In Gas + Sol, significantly higher unsaturated fatty acids (FA18.1- ω 9, FA20.3- ω 6, FA20.4- ω 6, FA20.5- ω 3, FA22.4- ω 6) and oxylipins (19-20-DiHDPA, 8-9-DiHETrE) were observed in delayed isolation samples compared to the fast isolation (Table 1). These fatty acids and oxylipins are in the arachidonic acid and eicosapentaenoic acid pathways, associated with inflammation and ageing-related diseases [39], and are oxidation sensitive [40, 41]. 15 min at room temperature led to longer oxygen exposure and potentially changed enzymatic activity in these muscle tissues, which contributed to oxidation and instability of the unsaturated fatty acids, and the generation of their downstream metabolites, *i.e.*, oxylipins [42, 43]. The higher lysophospholipids (Table 1), *i.e.*, LPE14.0, LPE16.1, LPE20.4, LPE22.4, LPG16.1, LPI20.4, LPI22.4, and LPI22.6, in 15 min delayed isolation muscle tissues might be due to the hydrolysis of cellular membrane induced by the longer time of oxidation exposure and oxidative damage [44, 45], and/or tissue degeneration. Significantly increased pyruvate in Gas + Sol with delayed isolation (Table 2) may be due to the oxidation of lactate [46]. Creatine phosphate is considered as the “energy pool” in muscle cells and will be preferentially consumed under the condition of insufficient energy, and generate its downstream metabolite, creatine [47]. Higher creatine content in Gas + Sol with 15 min delayed isolation (Table 2) may be explained by the insufficient energy supply in muscle tissues post-dissection, and the consumption of creatine phosphate in the muscle cells before the muscle tissue is isolated and snap frozen [47, 48]. Quadr muscle was much more stable than Gas + Sol with 15 min delayed isolation, as namely only 3 metabolites, *i.e.*, 7-HDoHE, creatine, and PEA, were significantly affected. More altered metabolites were observed in EDL + TA with 15 min delayed isolation compared to both Gas + Sol and Quadr.

The increase in the number of significantly altered metabolites after delayed isolation in Gas + Sol muscle compared to Quadr muscle, may be due to the type I oxidative muscle (soleus) included in Gas + Sol, and type II glycolytic muscle of Quadr [49-51]. The

oxidative fibers mainly use aerobic respiration to provide ATP, and glycolytic fibers primarily use anaerobic glycolysis as their energy supply [52], which induced more oxidation in Gas + Sol than Quadr. The largest number of significantly altered metabolites was observed in EDL + TA, which may be due to the varied and unsystematic muscle type composition and fiber density in TA [53-55]. Kammoun *et al.* found 57% of type IIB, 3% of hybrid IIX fibers, and no hybrid IIX/IIB fibers were observed in TA [53]. However, Bloemberg *et al.* found mouse white tibialis anterior contained 12.1% hybrid fibers [54]. Lexell *et al.* revealed that in TA, the proportion of type I fibers and fiber density varied significantly but not systematically, and also differed significantly between individuals [55]. Similarly, also the fiber types of EDL muscle in *Ercc1^{Δ/-}* mice are altered in composition compared to normal wildtype controls, having reduced type IIA/IIX and increased type IIB[19]. These variations in TA tissue and/or in mice may have contributed to the observed metabolite alterations in EDL + TA with 15 min delayed isolation at room temperature. The different muscle type proportion may be responsible for the observed differences in the stability of metabolites in the three different kinds of muscle. Because of the observed instability of metabolites in muscle tissues with 15 min delayed isolation, fast muscle tissue collection will be preferred for our future sarcopenia study.

Simultaneous extraction of non-polar and polar metabolites

Table 1. The effect of sample collection speed on lipid metabolites stability in different muscle types (n=3)

	Gas+Sol	Quadr	EDL+TA		Gas+Sol	Quadr	EDL+TA
FA16.0	ns	ns	*	LEA	*	ns	*
FA18.0	ns	ns	ns	SEA	ns	ns	ns
FA18.1- ω 9	*	ns	*	1-AG & 2-AG	*	ns	ns
FA18.3- ω 3	ns	ns	ns	CDCA	ns	ns	ns
FA20.3- ω 6	*	ns	ns	GCA	ns	ns	ns
FA20.3- ω 9	ns	ns	ns	GCDCA	ns	ns	ns
FA20.4- ω 6	*	ns	ns	GDCA	ns	ns	ns
FA20.5- ω 3	**	ns	ns	GUDCA	ns	ns	ns
FA22.4- ω 6	*	ns	*	cLPA16.1	ns	ns	ns
FA22.5- ω 3	ns	ns	ns	cLPA18.0	ns	ns	ns
FA22.5- ω 6	ns	ns	ns	cLPA18.1	ns	ns	ns
FA22.6- ω 3	ns	ns	*	cLPA18.2	ns	ns	ns
10-HDoHE	ns	ns	ns	LPA14.0	ns	ns	ns
11-HDoHE	ns	ns	ns	LPA16.1	ns	ns	ns
11-HETE	ns	ns	ns	LPA18.0	ns	ns	ns
12-13-DiHOME	ns	ns	ns	LPA18.1	ns	ns	ns
12-HEPE	ns	ns	***	LPA18.2	ns	ns	ns
13-14dihydro-15k-PGD2	ns	ns	ns	LPA20.4	ns	ns	*
13-14dihydro-15k-PGE2	ns	ns	*	LPA22.4	ns	ns	ns
13-14dihydro-PGF2 α	ns	ns	ns	LPE14.0	*	ns	ns
13-HODE	ns	ns	ns	LPE16.0	ns	ns	ns
14-15-DiHETrE	ns	ns	*	LPE16.1	*	ns	*
14-HDoHE	ns	ns	ns	LPE18.0	ns	ns	ns
8iso-PGE1	ns	ns	*	LPE18.1	ns	ns	*
8iso-PGF1 α	ns	ns	ns	LPE18.2	ns	ns	*
15S-HETrE	ns	ns	ns	LPE18.3	ns	ns	*
17-HDoHE	ns	ns	ns	LPE20.3	ns	ns	**
18-HEPE	ns	ns	***	LPE20.4	*	ns	*
19-20-DiHDPA	*	ns	**	LPE20.5	ns	ns	ns
1a-1b-dihomo-PGF2 α	ns	ns	ns	LPE22.4	*	ns	*
20-HETE	ns	ns	*	LPE22.5	ns	ns	ns

5-HETE	ns	ns	ns	LPE22.6	ns	ns	*
5-iPF2 α -VI	ns	ns	ns	LPG14.0	ns	ns	*
7-HDoHE	ns	*	ns	LPG16.0	ns	ns	ns
8-12-iso-iPF2 α -VI	ns	ns	ns	LPG16.1	*	ns	ns
8-9-DiHETrE	*	ns	*	LPG18.0	ns	ns	ns
8-HDoHE	ns	ns	ns	LPG18.1	ns	ns	ns
8-HETE	ns	ns	ns	LPG18.2	ns	ns	ns
8iso-15R-PGF2 α	ns	ns	ns	LPG20.3	ns	ns	*
8iso-PGE2	ns	ns	ns	LPG20.4	ns	ns	ns
8iso-PGF2 α	ns	ns	ns	LPG22.4	ns	ns	ns
8S-HETrE	ns	ns	ns	LPI16.1	ns	ns	*
9-10-13-TriHOME	ns	ns	ns	LPI18.0	ns	ns	ns
9-10-DiHOME	ns	ns	ns	LPI18.1	ns	ns	ns
9-HEPE	ns	ns	*	LPI18.2	ns	ns	*
9-HETE	ns	ns	ns	LPI20.4	*	ns	*
9-HODE	ns	ns	ns	LPI22.4	*	ns	*
iPF2 α -IV	ns	ns	ns	LPI22.6	*	ns	ns
PGD2	ns	ns	ns	LPS18.1	ns	ns	**
PGD3	ns	ns	ns	LPS18.2	ns	ns	**
PGE2	ns	ns	ns	LPS20.4	ns	ns	***
PGF2 α	ns	ns	*	LPS22.4	ns	ns	**
TXB2	ns	ns	ns	LPS22.6	*	ns	*
AEA	*	ns	*				
PEA	ns	*	ns				
OEA	ns	ns	ns				

Note: ns means no significant difference, * means $p < 0.05$, ** means $p < 0.01$, *** means $p < 0.001$. Orange background color means significantly increased; Blue background color means significantly decreased.

Simultaneous extraction of non-polar and polar metabolites

Table 2. The effect of sample collection speed on stability of energy metabolites, amino acids, and amines in different muscle types (n=3)

<i>Energy metabolites</i>							
	Gas+Sol	Quadr	EDL+TA		Gas+Sol	Quadr	EDL+TA
Acetyl-CoA	ns	ns	**	IMP	ns	ns	ns
Adenosine	**	ns	***	Creatine	*	*	ns
ADP	ns	ns	*	Inosine	ns	ns	ns
AMP	ns	ns	ns	α -Ketoglutarate	*	ns	ns
Ascorbic-acid	ns	ns	ns	6-phosphogluconic-acid	ns	ns	*
ATP	ns	ns	**	Malate	ns	ns	ns
cAMP	ns	ns	*	GTP	ns	ns	**
CDP	ns	ns	ns	Guanosine	ns	ns	ns
cis-Aconitate	ns	ns	ns	Oxiglutathione	ns	ns	ns
CMP	ns	ns	ns	Phosphoenolpyruvate	ns	ns	ns
CTP	ns	ns	ns	Pyruvate	**	ns	*
Cytidine	ns	ns	ns	Succinate	ns	ns	*
Dihydroxyacetone-P	ns	ns	*	UDP	ns	ns	ns
Fructose-6-P	ns	ns	ns	UMP	ns	ns	*
GABA	*	ns	ns	Uridine	ns	ns	**
GDP	ns	ns	ns	UTP	ns	ns	*
Glucose	ns	ns	ns	Xanthine	*	ns	**
Glucose-1-P	ns	ns	ns	Glycerate-3-P	ns	ns	ns
Glucose-6-P	ns	ns	ns	GMP	ns	ns	**
Glyceraldehyde-3-P	ns	ns	ns	Hypoxanthine	*	ns	ns
<i>Amino acids and amines</i>							
Alanine	ns	ns	ns	Methionine	ns	ns	*
Arginine	ns	ns	ns	Phenylalanine	*	ns	ns
Asparagine	ns	ns	ns	Proline	ns	ns	ns
Aspartic-acid	ns	ns	*	Serine	ns	ns	ns
Lysine	ns	ns	ns	Spermidine	ns	ns	ns
Creatinine	ns	ns	ns	Tyrosine	ns	ns	ns
Glutamic-acid	ns	ns	ns	Valine	ns	ns	ns
Glutamine	ns	ns	ns	Threonine	ns	ns	ns
Glycine	ns	ns	*	Ornithine	ns	ns	ns
Histidine	ns	ns	ns	4-Hydroxyproline	*	ns	ns
Leucine	ns	ns	ns	Tryptophan	ns	ns	ns

Note: ns means no significant difference, * means $p < 0.05$, ** means $p < 0.01$, *** means $p < 0.001$. Orange background color means significantly increased; Blue background color means significantly decreased.

4. Conclusion

Four extraction methods (BD, BMC, BMW, BMMW) were compared and evaluated to find the optimal sample preparation method for the simultaneous extraction of targeted non-polar and polar metabolites from limited amount of muscle tissues. The optimal method, BMMW, had an acceptable matrix effect (close to 1.0) for all metabolites and showed the highest extraction recovery for all types of metabolites, with the best performance of all methods studied for 63% of the signaling lipids and 81% of the polar metabolites. BMMW was used for profiling mouse muscle tissues with quantities as small as 5 mg (dry weight). Our study of sample collection protocols found that fast (<15 min) muscle tissue collection is crucial for metabolite stability. The developed sensitive sample preparation method and fast muscle tissue isolation method will be utilized for future metabolomics mechanistic studies of sarcopenia and animal model studies to evaluate treatments to prevent this syndrome.

Acknowledgements

We thank Kimberly Smit, Renata Brandt, Sander Barnhoorn, and the animal caretakers for general assistance with mouse experiments.

Funding: This work was supported by the Netherlands Organisation for Scientific Research (NWO) in the Building Blocks of Life [grant number 737.016.015]; the China Scholarship Council (CSC) [No. 201706320322]. JH was additionally supported by the European Research Council Advanced Grant Dam2Age, NIH grant (PO1 AG017242), the Deutsche Forschungsgemeinschaft - Project-ID 73111208 - SFB 829, JH and WV by ZonMW Memorabel (733050810), and EJP-RD TC-NER RD20-113, and JH, WV and YR by ONCODE (Dutch Cancer Society).

Reference

- [1] V. Santilli, A. Bernetti, M. Mangone, and M. Paoloni, Clinical definition of sarcopenia. Clinical cases in mineral and bone metabolism : the official journal of the Italian Society of Osteoporosis, Mineral Metabolism, and Skeletal Diseases, (11) 2014. 177-180.
- [2] R.A. Fielding, B. Vellas, W.J. Evans, S. Bhasin, J.E. Morley, A.B. Newman, G. Abellan van Kan, S. Andrieu, J. Bauer, D. Breuille, T. Cederholm, J. Chandler, C. De Meynard, L. Donini, T. Harris, A. Kannt, F. Keime Guibert, G. Onder, D. Papanicolaou, Y. Rolland, D. Rooks, C. Sieber, E. Souhami, S. Verlaan, and M. Zamboni, Sarcopenia: an undiagnosed condition in older adults.

- Current consensus definition: prevalence, etiology, and consequences. International working group on sarcopenia. *J Am Med Dir Assoc*, (12) 2011. 249-56.
- [3] S. von Haehling, J.E. Morley, and S.D. Anker, An overview of sarcopenia: facts and numbers on prevalence and clinical impact. *J Cachexia Sarcopenia Muscle*, (1) 2010. 129-133.
- [4] J.Y. Kwak and K.-S. Kwon, Pharmacological Interventions for Treatment of Sarcopenia: Current Status of Drug Development for Sarcopenia. *Annals of geriatric medicine and research*, (23) 2019. 98-104.
- [5] A. Zhang, H. Sun, G. Yan, P. Wang, and X. Wang, Metabolomics for Biomarker Discovery: Moving to the Clinic. *BioMed research international*, (2015) 2015. 354671-354671.
- [6] C. Dalle, A.I. Ostermann, T. Konrad, C. Coudy-Gandilhon, A. Decourt, J.C. Barthelemy, F. Roche, L. Feasson, A. Mazur, D. Bechet, N.H. Schebb, and C. Gladine, Muscle Loss Associated Changes of Oxylipin Signatures During Biological Aging: An Exploratory Study From the PROOF Cohort. *J Gerontol A Biol Sci Med Sci*, (74) 2019. 608-615.
- [7] S.P.B. Caligiuri, M. Parikh, A. Stamenkovic, G.N. Pierce, and H.M. Aukema, Dietary modulation of oxylipins in cardiovascular disease and aging. *American Journal of Physiology-Heart and Circulatory Physiology*, (313) 2017. H903-H918.
- [8] C. Mo, Y. Du, and T.M. O'Connell, Applications of Lipidomics to Age-Related Musculoskeletal Disorders. *Current Osteoporosis Reports*, (19) 2021. 151-157.
- [9] O. Pastoris, F. Boschi, M. Verri, P. Baiardi, G. Felzani, J. Vecchiet, M. Dossena, and M. Catapano, The effects of aging on enzyme activities and metabolite concentrations in skeletal muscle from sedentary male and female subjects. *Exp Gerontol*, (35) 2000. 95-104.
- [10] K.S. Nair, Aging muscle. *American Journal of Clinical Nutrition*, (81) 2005. 953-963.
- [11] B.S. Kirby, A.R. Crecelius, W.F. Voyles, and F.A. Dinunno, Impaired Skeletal Muscle Blood Flow Control With Advancing Age in Humans Attenuated ATP Release and Local Vasodilation During Erythrocyte Deoxygenation. *Circulation Research*, (111) 2012. 220-U245.
- [12] S. Fujita and E. Volpi, Amino acids and muscle loss with aging. *Journal of Nutrition*, (136) 2006. 277s-280s.
- [13] M. Sheffield-Moore, D. Paddon-Jones, and R.J. Urban, Amino acid supplementation and skeletal muscle metabolism in ageing populations. *Hormone Research*, (66) 2006. 93-97.
- [14] W.P. Vermeij, J.H. Hoeijmakers, and J. Pothof, Genome Integrity in Aging: Human Syndromes, Mouse Models, and Therapeutic Options. *Annu Rev Pharmacol Toxicol*, (56) 2016. 427-45.
- [15] M.E. Dolle, R.V. Kuiper, M. Roodbergen, J. Robinson, S. de Vlugt, S.W. Wijnhoven, R.B. Beems, L. de la Fonteyne, P. de With, I. van der Pluijm, L.J. Niedernhofer, P. Hasty, J. Vijg, J.H. Hoeijmakers, and H. van Steeg, Broad segmental progeroid changes in short-lived *Ercc1(-/Delta7)* mice. *Pathobiol Aging Age Relat Dis*, (1) 2011.
- [16] G. Weeda, I. Donker, J. de Wit, H. Morreau, R. Janssens, C.J. Vissers, A. Nigg, H. van Steeg, D. Bootsma, and J.H. Hoeijmakers, Disruption of mouse *ERCC1* results in a novel repair syndrome with growth failure, nuclear abnormalities and senescence. *Curr Biol*, (7) 1997. 427-39.
- [17] E.L. de Graaf, W.P. Vermeij, M.C. de Waard, Y. Rijksen, I. van der Pluijm, C.C. Hoogenraad, J.H. Hoeijmakers, A.F. Altelaar, and A.J. Heck, Spatio-temporal analysis of molecular determinants of neuronal degeneration in the aging mouse cerebellum. *Mol Cell Proteomics*, (12) 2013. 1350-62.
- [18] M.J. Yousefzadeh, J. Zhao, C. Bukata, E.A. Wade, S.J. McGowan, L.A. Angelini, M.P. Bank, A.U. Gurkar, C.A. McGuckian, M.F. Calubag, J.I. Kato, C.E. Burd, P.D. Robbins, and L.J. Niedernhofer, Tissue specificity of senescent cell accumulation during physiologic and accelerated aging of mice. *Aging Cell*, (19) 2020. e13094.
- [19] K. Alyodawi, W.P. Vermeij, S. Omairi, O. Kretz, M. Hopkinson, F. Solagna, B. Joch, R.M.C. Brandt, S. Barnhoorn, N. van Vliet, Y. Ridwan, J. Essers, R. Mitchell, T. Morash, A. Pasternack, O. Ritvos, A. Matsakas, H. Collins-Hooper, T.B. Huber, J.H.J. Hoeijmakers, and K. Patel, Compression of morbidity in a progeroid mouse model through the attenuation of myostatin/activin signalling. *J Cachexia Sarcopenia Muscle*, (10) 2019. 662-686.
- [20] W.P. Vermeij, M.E.T. Dollé, E. Reiling, D. Jaarsma, C. Payan-Gomez, C.R. Bombardieri, H. Wu, A.J.M. Roks, S.M. Botter, B.C. van der Eerden, S.A. Youssef, R.V. Kuiper, B. Nagarajah,

- C.T. van Oostrom, R.M.C. Brandt, S. Barnhoorn, S. Imholz, J.L.A. Pennings, A. de Bruin, Á. Gyenis, J. Pothof, J. Vijg, H. van Steeg, and J.H.J. Hoeijmakers, Restricted diet delays accelerated ageing and genomic stress in DNA-repair-deficient mice. *Nature*, (537) 2016. 427-431.
- [21] L.J. Niedernhofer, G.A. Garinis, A. Raams, A.S. Lalai, A.R. Robinson, E. Appeldoorn, H. Odijk, R. Oostendorp, A. Ahmad, and W. Van Leeuwen, A new progeroid syndrome reveals that genotoxic stress suppresses the somatotroph axis. *Nature*, (444) 2006. 1038-1043.
- [22] J.A. Marteijn, H. Lans, W. Vermeulen, and J.H. Hoeijmakers, Understanding nucleotide excision repair and its roles in cancer and ageing. *Nature reviews Molecular cell biology*, (15) 2014. 465-481.
- [23] H. Lans, J.H.J. Hoeijmakers, W. Vermeulen, and J.A. Marteijn, The DNA damage response to transcription stress. *Nature Reviews Molecular Cell Biology*, (20) 2019. 766-784.
- [24] C.Z. Ulmer, C.M. Jones, R.A. Yost, T.J. Garrett, and J.A. Bowden, Optimization of Folch, Bligh-Dyer, and Matyash sample-to-extraction solvent ratios for human plasma-based lipidomics studies. *Analytica Chimica Acta*, (1037) 2018. 351-357.
- [25] O. Vvedenskaya, Y. Wang, J.M. Ackerman, O. Knittelfelder, and A. Shevchenko, Analytical challenges in human plasma lipidomics: A winding path towards the truth. *TrAC Trends in Analytical Chemistry*, (120) 2019. 115277.
- [26] J. Medina, V. van der Velpen, T. Teav, Y. Guitton, H. Gallart-Ayala, and J. Ivanisevic, Single-Step Extraction Coupled with Targeted HILIC-MS/MS Approach for Comprehensive Analysis of Human Plasma Lipidome and Polar Metabolome. *Metabolites*, (10) 2020.
- [27] L. Löfgren, M. Ståhlman, G.-B. Forsberg, S. Saarinen, R. Nilsson, and G.I. Hansson, The BUMÉ method: a novel automated chloroform-free 96-well total lipid extraction method for blood plasma. *Journal of lipid research*, (53) 2012. 1690-1700.
- [28] A. Di Zazzo, W. Yang, M. Coassin, A. Micera, M. Antonini, F. Piccinni, M. De Piano, I. Kohler, A.C. Harms, T. Hankemeier, S. Boinini, and A. Mashaghi, Signaling lipids as diagnostic biomarkers for ocular surface cicatrizing conjunctivitis. *Journal of Molecular Medicine-Jmm*, (98) 2020. 751-760.
- [29] R.D.A.M. Alves, A.D. Dane, A. Harms, K. Strassburg, R.M. Seifar, L.B. Verdijk, S. Kersten, R. Berger, T. Hankemeier, and R.J. Vreeken, Global profiling of the muscle metabolome: method optimization, validation and application to determine exercise-induced metabolic effects. *Metabolomics*, (11) 2014. 271-285.
- [30] V. Shinin, B. Gayraud-Morel, and S. Tajbakhsh, Template DNA-strand co-segregation and asymmetric cell division in skeletal muscle stem cells. *Methods Mol Biol*, (482) 2009. 295-317.
- [31] M.R. Buijink, M. van Weeghel, M.C. Gulersonmez, A.C. Harms, J.H.T. Rohling, J.H. Meijer, T. Hankemeier, and S. Michel, The influence of neuronal electrical activity on the mammalian central clock metabolome. *Metabolomics*, (14) 2018. 122.
- [32] N. Drouin, J. Pezzatti, Y. Gagnebin, V. González-Ruiz, J. Schappler, and S. Rudaz, Effective mobility as a robust criterion for compound annotation and identification in metabolomics: Toward a mobility-based library. *Analytica Chimica Acta*, (1032) 2018. 178-187.
- [33] C. Reichardt and T. Welton, *Solvents and solvent effects in organic chemistry*. 2011: John Wiley & Sons.
- [34] *Chapter 3 Lipid extraction procedures*, in *Laboratory Techniques in Biochemistry and Molecular Biology*, T.S. Work and E. Work, Editors. 1972, Elsevier. p. 347-353.
- [35] E.W. Becker, The roles of ATP in the dynamics of the actin filaments of the cytoskeleton. *Biol Chem*, (387) 2006. 401-6.
- [36] C. Bruno, F. Patin, C. Bocca, L. Nadal-Desbarats, F. Bonnier, P. Reynier, P. Emond, P. Vourc'h, K. Joseph-Delafont, P. Corcia, C.R. Andres, and H. Blasco, The combination of four analytical methods to explore skeletal muscle metabolomics: Better coverage of metabolic pathways or a marketing argument? *Journal of Pharmaceutical and Biomedical Analysis*, (148) 2018. 273-279.
- [37] S. Bellmaine, A. Schnellbaecher, and A. Zimmer, Reactivity and degradation products of tryptophan in solution and proteins. *Free Radical Biology and Medicine*, (160) 2020. 696-718.
- [38] J.C. Schoeman, A.C. Harms, M. van Weeghel, R. Berger, R.J. Vreeken, and T. Hankemeier, Development and application of a UHPLC-MS/MS metabolomics based comprehensive systemic

- and tissue-specific screening method for inflammatory, oxidative and nitrosative stress. *Anal Bioanal Chem*, (410) 2018. 2551-2568.
- [39] U.N. Das, Ageing: Is there a role for arachidonic acid and other bioactive lipids? A review. *Journal of Advanced Research*, (11) 2018. 67-79.
- [40] F. Sardenne, E. Puccinelli, M. Vagner, L. Pecquerie, A. Bideau, F. Le Grand, and P. Soudant, Post-mortem storage conditions and cooking methods affect long-chain omega-3 fatty acid content in Atlantic mackerel (*Scomber scombrus*). *Food Chem*, (359) 2021. 129828.
- [41] R.J. Hsieh and J.E. Kinsella, Oxidation of polyunsaturated fatty acids: mechanisms, products, and inhibition with emphasis on fish. *Adv Food Nutr Res*, (33) 1989. 233-341.
- [42] N. Kaur, V. Chugh, and A.K. Gupta, Essential fatty acids as functional components of foods- a review. *Journal of Food Science and Technology-Mysore*, (51) 2014. 2289-2303.
- [43] H. Suganuma, C.T. Collins, A.J. McPhee, S. Leemaqz, G. Liu, C.C. Andersen, D. Bonney, and R.A. Gibson, Effect of parenteral lipid emulsion on preterm infant PUFAs and their downstream metabolites. *Prostaglandins Leukotrienes and Essential Fatty Acids*, (164) 2021.
- [44] T. El-Bacha and A.G. Torres, *Phospholipids: Physiology*, in *Encyclopedia of Food and Health*, B. Caballero, P.M. Finglas, and F. Toldrá, Editors. 2016, Academic Press: Oxford. p. 352-359.
- [45] I.V. Kondakova, E.V. Borunov, and E.V. Antipova, [Activation of phospholipase hydrolysis in the process of oxidative cell damage]. *Biulleten' eksperimental'noi biologii i meditsiny*, (112) 1991. 285-287.
- [46] G.A. Brooks, H. Dubouchaud, M. Brown, J.P. Sicurello, and C.E. Butz, Role of mitochondrial lactate dehydrogenase and lactate oxidation in the intracellular lactate shuttle. *Proc Natl Acad Sci U S A*, (96) 1999. 1129-34.
- [47] R.A. Rhoades and D.R. Bell, *Medical physiology: Principles for clinical medicine*. 2012: Lippincott Williams & Wilkins.
- [48] D.M. Vasudevan, S. Sreekumari, and K. Vaidyanathan, *Textbook of biochemistry for medical students*. 2019: Jaypee brothers Medical publishers.
- [49] R.A. Jacobs, V. Diaz, L. Soldini, T. Haider, M. Thomassen, N.B. Nordsborg, M. Gassmann, and C. Lundby, Fast-Twitch Glycolytic Skeletal Muscle Is Predisposed to Age-Induced Impairments in Mitochondrial Function. *Journals of Gerontology Series a-Biological Sciences and Medical Sciences*, (68) 2013. 1010-1022.
- [50] J.T. Shu, Q. Xiao, Y.J. Shan, M. Zhang, Y.J. Tu, G.G. Ji, Z.W. Sheng, and J.M. Zou, Oxidative and glycolytic skeletal muscles show marked differences in gene expression profile in Chinese Qingyuan partridge chickens. *Plos One*, (12) 2017.
- [51] T. Soukup, G. Zacharová, and V. Smerdu, Fibre type composition of soleus and extensor digitorum longus muscles in normal female inbred Lewis rats. *Acta Histochem*, (104) 2002. 399-405.
- [52] L.M. Biga, S. Dawson, A. Harwell, R. Hopkins, J. Kaufmann, M. LeMaster, P. Matern, K. Morrison-Graham, D. Quick, and J. Runyeon, *Anatomy & physiology*. 2020.
- [53] M. Kammoun, I. Cassar-Malek, B. Meunier, and B. Picard, A simplified immunohistochemical classification of skeletal muscle fibres in mouse. *European journal of histochemistry : EJH*, (58) 2014. 2254-2254.
- [54] D. Bloemberg and J. Quadriatero, Rapid determination of myosin heavy chain expression in rat, mouse, and human skeletal muscle using multicolor immunofluorescence analysis. *PloS one*, (7) 2012. e35273.
- [55] J. Lexell, J.C. Jarvis, J. Currie, D.Y. Downham, and S. Salmons, Fibre type composition of rabbit tibialis anterior and extensor digitorum longus muscles. *Journal of anatomy*, (185 (Pt 1)) 1994. 95-101.

Supplementary Information

Table S1. The information of lipid ISTDs

Name	Concentration (mM)	Precursor Mass (M/Z)	Fragment Mass (M/Z)	Retention Time (min)	Class
<i>Analyzed by low pH LC-MS/MS method</i>					
DCA-d4	1.00	395.3	349.1	10.2	Bile Acids & Steroid
GCA-d4	1.00	468.3	74.05	5.5	Bile Acids & Steroid
UDCA-d4	1.00	395.3	395.3	8.1	Bile Acids & Steroid
GUDCA-d5	1.00	453.3	74.1	5	Bile Acids & Steroid
SEA-d3	0.10	331.3	62.2	13.72	Endocannabinoids
OEA-d4	0.10	330.3	66.2	13.35	Endocannabinoids
PEA-d4	0.10	304.3	62.2	13.23	Endocannabinoids
2-AG-d8	0.26	387.3	294.2	13.21	Endocannabinoids
10-NO ₂ -OA-d17	2.90	343.2	183.2	13.2	Fatty acids
FA 18:1- ω 9-d17	3.34	298.1	298.1	13.8	Fatty acids
FA 22:6- ω 3-d5	1.50	332.1	288.4	13.4	Fatty acids
FA 20:4- ω 6-d8	32.00	311.1	267.2	13.47	Fatty acids
14,15-DiHETrE-d11	0.29	348.2	207.1	9.8	Oxylipins
5-iPF _{2α} -VI-d11	0.27	364.2	115.05	3.9	Oxylipins
8,12-iPF _{2α} -IV-d11	0.27	364.21	115.05	5.9	Oxylipins
12,13-DiHOME-d4	0.31	317.2	185.1	9.3	Oxylipins
8iso-PGE ₂ -d4	0.28	355.3	275.25	5.42	Oxylipins
8iso-PGF _{2α} -d4	0.28	357.3	197.15	4.75	Oxylipins
9,10-DiHOME-d4	0.31	317.2	203.1	9.5	Oxylipins
9-HODE-d4	0.33	299.2	172.1	11.1	Oxylipins
LTB ₄ -d4	0.29	339.5	197.1	9.2	Oxylipins
PGE ₂ -d4	0.28	355.3	275.25	5.42	Oxylipins
PGF _{2α} -d4	0.28	357.3	197.15	4.75	Oxylipins
TXB ₂ -d4	0.27	373.5	173.3	3.7	Oxylipins
20-HETE-d6	0.31	325.2	279.2	10.6	Oxylipins
12-HETE-d8	0.30	327.2	184.1	11.7	Oxylipins
5-HETE-d8	0.30	327.1	116.15	12.1	Oxylipins
<i>Analyzed by high pH LC-MS/MS method</i>					
FA 18:1- ω 9-d17	3.34	298.2	298.2	4.31	Fatty acids
FA 22:6- ω 3-d5	1.50	332.3	288.25	4.11	Fatty acids
cLPA 17:0	2.31	405.2	269.25	5.53	Lysophospholipids & Sphingolipids
PAF 16:0	9.00	572.2	59	6.68	Lysophospholipids & Sphingolipids

Simultaneous extraction of non-polar and polar metabolites

LPA 17:0	14.73	423.2	153.05	4.17	Lysophospholipids & Sphingolipids
LPE 17:1	10.73	464.4	267.35	5.35	Lysophospholipids & Sphingolipids
LPI 17:1	0.57	583.4	267.3	4.59	Lysophospholipids & Sphingolipids
LPS 17:1	9.82	508.4	153.2	4.10	Lysophospholipids & Sphingolipids
Sph-1-P 17:0	2.72	366	79.05	3.60	Lysophospholipids & Sphingolipids
Sph-1-P 17:1	2.74	364	79	3.31	Lysophospholipids & Sphingolipids

Table S2. The information of amino acids and amines ISTDs

Name	Concentration (mg/mL)	Molar mass (M/Z)	Retention Time (min)	Class
<i>Analyzed by HILIC-MS method</i>				
Asparagine- ¹³ C ₄ , ¹⁵ N ₂	0.5	137.0537	12.84	Amine
Glutamate- ¹³ C ₅ , d ₃ , ¹⁵ N	0.5	157.0911	8.38	Amino acid
Isoleucine- ¹³ C, ¹⁵ N	0.5	132.0877	7.93	Amino acid
Valine- ¹³ C ₅	0.5	121.0885	6.89	Amino acid
Leucine-d ₃	0.5	133.1062	7.64	Amino acid
<i>Analyzed by CE-MS method</i>				
Aspartate- ¹³ C ₄ , d ₃ , ¹⁵ N	0.5	142.0448	14.10	Amino acid
Glutamate- ¹³ C ₅ , d ₅ , ¹⁵ N	0.5	159.0604	12.80	Amino acid
Glutamine- ¹³ C ₅	0.5	152.0764	12.70	Amine
Glycine-d ₂	0.5	78.0322	9.80	Amino acid
Isoleucine- ¹³ C, ¹⁵ N	0.5	134.0877	11.02	Amino acid
Tryptophan- ¹³ C ₁₁ , ¹⁵ N ₂	0.5	218.0972	12.50	Amino acid
Valine- ¹³ C ₅	0.5	123.0863	11.40	Amino acid

Table S3. The information of energy metabolites ISTDs

Name	Concentration	Molar mass (M/Z)	Retention Time (min)	Class
<i>Spiking before sample extraction (for sample extraction method evaluation)</i>				
ATP- ¹³ C ₁₀ , ¹⁵ N ₅	10 mg/mL	520.9885	12.74	Energy metabolites
AMP- ¹³ C ₁₀ , ¹⁵ N ₅	10 mg/mL	361.0558	7.07	Energy metabolites
UTP- ¹³ C ₉ , ¹⁵ N ₂	10 mg/mL	493.9613	13.90	Energy metabolites
<i>Spiking before MS analysis (only for response ratio calculation)</i>				
Fumarate-d ₂	500 mM	117.0162	13.10	Energy metabolites
Pyruvate- ¹³ C ₃	500 mM	90.0188	6.45	Energy metabolites
Succinate-d ₄	500 mM	121.0444	7.95	Energy metabolites
UMP- ¹⁵ N ₂	500 mM	325.0227	7.10	Energy metabolites

Table S4. Detected lipid metabolites in mouse muscle samples

Name	Precursor Mass (M/Z)	Fragment Mass (M/Z)	Retention Time (min)	ChEBI ID	ISTD	Class
<i>Analyzed by low pH LC-MS/MS method</i>						
CDCA	391.2	373.25	10	16755	DCA-d4	Bile Acids & Steroid
GCA	464.2	74.1	5.5	17687	GCA-d4	Bile Acids & Steroid
GCDCA	448.21	74	8.3	36274	GUDCA-d5	Bile Acids & Steroid
GDCA	448.22	74	8.7	27471	GUDCA-d5	Bile Acids & Steroid
GUDCA	448.2	74	5	89929	GUDCA-d5	Bile Acids & Steroid
1-AG and 2-AG (two peaks merged to one)	379.21	287	13.3	34071 and 52392	2-AG-d8	Endocannabinoids
AEA	348	62	13	2700	SEA-d3	Endocannabinoids
LEA	324	62	12.9	64032	SEA-d3	Endocannabinoids
OEA	326	62	13.4	71466	OEA-d4	Endocannabinoids
PEA	300	62	13.2	71464	PEA-d4	Endocannabinoids
SEA	328	62	13.7	85299	SEA-d3	Endocannabinoids
FA16.0	255.2	237.2	13.8	15756	FA 18:1- ω 9-d17	Fatty acids
FA18.0	283.2	265.2	14.1	28842	FA 18:1- ω 9-d17	Fatty acids
FA18.1- ω 9	281.1	263.2	13.8	16196	FA 18:1- ω 9-d17	Fatty acids
FA20.3- ω 6	305.1	261	13.7	NA	FA 20:4- ω 6-d8	Fatty acids
FA20.3- ω 9	305.1	261	13.8	72865	FA 20:4- ω 6-d8	Fatty acids
FA20.4- ω 6	303	259	13.5	15843	FA 20:4- ω 6-d8	Fatty acids
FA20.5- ω 3	301.1	257.2	13.3	28364	FA 20:4- ω 6-d8	Fatty acids
FA22.6- ω 3	327.1	283.1	13.4	28125	FA 22:6- ω 3-d5	Fatty acids
10-HDoHE	343.21	153.1	11.8	72640	12-HETE-d8	Oxylipins
11-HDoHE	343.2	121.1	11.9	72794	12-HETE-d8	Oxylipins
11-HETE	319.2	167.1	11.6	72606	12-HETE-d8	Oxylipins
12,13-DiHOME	313.2	183.1	9.3	72665	12,13-DiHOME-d4	Oxylipins
12-HEPE	317.2	179.1	10.8	NA	12-HETE-d8	Oxylipins
13,14dihydro-15k-PGD ₂	351.21	175.1	6.6	72603	PGE ₂ -d4	Oxylipins
13,14dihydro-15k-PGE ₂	351.2	175.1	5.7	15550	PGE ₂ -d4	Oxylipins
13,14dihydro-PGF _{2α}	355.2	311.3	5.4	63976	PGF _{2α} -d4	Oxylipins
13-HODE	295.2	195.2	11	72639	9-HODE-d4	Oxylipins
14,15-DiHETrE	337.2	207.1	9.8	63966	14,15-DiHETrE-d11	Oxylipins
14-HDoHE	343.2	205.1	11.7	72647	12-HETE-d8	Oxylipins

Simultaneous extraction of non-polar and polar metabolites

15S-HETrE	321.2	221.1	12	88348	5-HETE-d8	Oxylipins
17-HDoHE	343.2	281.2	11.2	72637	12-HETE-d8	Oxylipins
18-HEPE	317.2	299.2	10.4	72802	12-HETE-d8	Oxylipins
19,20-DiHDPa	361.2	273.2	9.9	72657	14,15-DiHETrE-d11	Oxylipins
1a,1b-dihomo-PGF _{2α}	381.1	337.45	7.3	NA	PGF _{2α} -d4	Oxylipins
20-HETE	319.2	289.2	10.6	34306	20-HETE-d6	Oxylipins
5-HETE	319.2	115.15	12.3	28209	5-HETE-d8	Oxylipins
5-iPF _{2α} -VI	353.2	115.05	4	140933	5-iPF _{2α} -VI-d11	Oxylipins
7-HDoHE	343.2	281.2	12.1	72623	12-HETE-d8	Oxylipins
8-12-iso-iPF _{2α} -VI	353.21	115.05	6	NA	8,12-iPF _{2α} -IV-d11	Oxylipins
8-9-DiHETrE	337.2	127.2	10.3	63970	14,15-DiHETrE-d11	Oxylipins
8-HDoHE	343.2	189.1	12.1	72610	12-HETE-d8	Oxylipins
8-HETE	319.2	155.1	11.8	34486	5-HETE-d8	Oxylipins
8iso-15R-PGF _{2α}	353.1	193.1	3.5	NA	8iso-PGF _{2α} -d4	Oxylipins
8iso-PGE ₁	353.2	317.2	4.7	NA	8iso-PGE ₂ -d4	Oxylipins
8iso-PGE ₂	351.1	271.15	4.5	131888	8iso-PGE ₂ -d4	Oxylipins
8iso-PGF _{1α}	355.2	311.1	4.5	NA	8iso-PGF _{2α} -d4	Oxylipins
8iso-PGF _{2α}	353.1	193.1	3.7	34509	8iso-PGF _{2α} -d4	Oxylipins
8(S)-HETrE	321.2	303.2	12.3	140473	12-HETE-d8	Oxylipins
9-10-13-TriHOME	329.2	171.1	4.4	NA	12-HETE-d8	Oxylipins
9-10-DiHOME	313.2	201.05	9.6	72663	9,10-DiHOME-d4	Oxylipins
9-HEPE	317.2	167.25	10.9	89570	12-HETE-d8	Oxylipins
9-HETE	319.21	167.1	12	72786	12-HETE-d8	Oxylipins
9-HODE	295.21	171.1	11.1	72651	9-HODE-d4	Oxylipins
iPF _{2α} -IV	353.3	127.1	3.2	NA	5-iPF _{2α} -VI-d11	Oxylipins
PGD ₂	351.1	271.15	5.1	15555	PGE ₂ -d4	Oxylipins
PGD ₃	349.2	269.2	3.6	34939	PGE ₂ -d4	Oxylipins
PGE ₂	351.1	271.15	4.8	15551	PGE ₂ -d4	Oxylipins
PGF _{2α}	353.1	193.1	4.6	28031	PGF _{2α} -d4	Oxylipins
TXB ₂	369.2	169.1	3.8	15553	TXB ₂ -d4	Oxylipins
Analyzed by high pH LC-MS/MS method						
FA18:3-ω3	277.1	233.15	3.9	27432	FA 18:1-ω9-d17_	Fatty acids
FA22:4-ω6	331.2	287.4	5.1	NA	FA 22:6-ω3-d5	Fatty acids
FA22:5-ω3	329.2	285.4	4.7	NA	FA 22:6-ω3-d5	Fatty acids
FA22:5-ω6	329.2	285.4	4.8	NA	FA 22:6-ω3-d5	Fatty acids
cLPA16.1	389.1	253	4.7	NA	cLPA 17:0	Lysophospholipids & Sphingolipids

cLPA18.0	419.1	283	5.9	NA	cLPA 17:0	Lysophospholipid s & Sphingolipids
cLPA18.1	417.2	281	5.4	62838	cLPA 17:0	Lysophospholipid s & Sphingolipids
cLPA18.2	415.1	279	5	NA	cLPA 17:0	Lysophospholipid s & Sphingolipids
LPA14.0	381.2	153.05	3.2	62833	LPA 17:0	Lysophospholipid s & Sphingolipids
LPA16.1	407.2	153.05	3.5	75070	LPA 17:0	Lysophospholipid s & Sphingolipids
LPA18.0	437.3	153.05	4.5	74850	LPA 17:0	Lysophospholipid s & Sphingolipids
LPA18.1	435.2	153.05	4.1	62837	LPA 17:0	Lysophospholipid s & Sphingolipids
LPA18.2	433.2	153.05	3.7	62834	LPA 17:0	Lysophospholipid s & Sphingolipids
LPA20.4	457	153.05	3.9	73792	LPA 17:0	Lysophospholipid s & Sphingolipids
LPA22.4	485.2	153.05	4.4	NA	LPA 17:0	Lysophospholipid s & Sphingolipids
LPE14.0	424.4	196.15	4.7	NA	LPE 17:1	Lysophospholipid s & Sphingolipids
LPE16.0	452.4	196.15	5.5	73134	LPE 17:1	Lysophospholipid s & Sphingolipids
LPE16.1	450.4	196.15	5	NA	LPE 17:1	Lysophospholipid s & Sphingolipids
LPE18.0	480.4	196.25	6.3	83047	LPE 17:1	Lysophospholipid s & Sphingolipids
LPE18.1	478.4	196.25	5.7	75168	LPE 17:1	Lysophospholipid s & Sphingolipids
LPE18.2	476.4	196.25	5.2	83058	LPE 17:1	Lysophospholipid s & Sphingolipids
LPE18.3	474.4	196.25	4.9	NA	LPE 17:1	Lysophospholipid s & Sphingolipids
LPE20.3	502.4	196.15	5.6	NA	LPE 17:1	Lysophospholipid s & Sphingolipids
LPE20.4	500.4	196.15	5.3	64395	LPE 17:1	Lysophospholipid s & Sphingolipids
LPE20.5	498.4	196.15	4.9	NA	LPE 17:1	Lysophospholipid s & Sphingolipids
LPE22.4	528.4	196.15	5.9	NA	LPE 17:1	Lysophospholipid s & Sphingolipids
LPE22.5	526.4	196.15	5.5	NA	LPE 17:1	Lysophospholipid s & Sphingolipids
LPE22.6	524.4	196.15	5.3	72747	LPE 17:1	Lysophospholipid s & Sphingolipids
LPG14.0	455.1	227.3	4.1	73092	LPI 17:1	Lysophospholipid s & Sphingolipids
LPG16.0	483.1	255.3	4.9	75376	LPI 17:1	Lysophospholipid s & Sphingolipids
LPG16.1	481.1	253.3	4.3	138795	LPI 17:1	Lysophospholipid s & Sphingolipids
LPG18.0	511.1	283.3	5.5	73091	LPI 17:1	Lysophospholipid s & Sphingolipids
LPG18.1	509.1	281.3	5	72952	LPI 17:1	Lysophospholipid s & Sphingolipids
LPG18.2	507.1	279.3	4.6	NA	LPI 17:1	Lysophospholipid s & Sphingolipids

Simultaneous extraction of non-polar and polar metabolites

LPG20.3	533.1	305.3	5	NA	LPI 17:1	Lysophospholipid s & Sphingolipids
LPG20.4	531.1	303.3	4.8	NA	LPI 17:1	Lysophospholipid s & Sphingolipids
LPG22.4	559.1	331.3	5.2	NA	LPI 17:1	Lysophospholipid s & Sphingolipids
LPI16.1	569.1	253.25	4.3	NA	LPI 17:1	Lysophospholipid s & Sphingolipids
LPI18.0	599.1	283.25	5.4	NA	LPI 17:1	Lysophospholipid s & Sphingolipids
LPI18.1	597.1	281.25	4.8	NA	LPI 17:1	Lysophospholipid s & Sphingolipids
LPI18.2	595.1	153.05	4.5	NA	LPI 17:1	Lysophospholipid s & Sphingolipids
LPI20.4	619.1	303.25	4.6	NA	LPI 17:1	Lysophospholipid s & Sphingolipids
LPI22.4	647.2	331.2	5.1	NA	LPI 17:1	Lysophospholipid s & Sphingolipids
LPI22.6	643.2	327.2	4.6	138564	LPI 17:1	Lysophospholipid s & Sphingolipids
LPS18.1	522.4	153.1	4.4	52649	LPS 17:1	Lysophospholipid s & Sphingolipids
LPS18.2	520.1	153.05	4.1	NA	LPS 17:1	Lysophospholipid s & Sphingolipids
LPS20.4	544.1	153.05	4.1	85435	LPS 17:1	Lysophospholipid s & Sphingolipids
LPS22.4	572.1	153.05	4.6	NA	LPS 17:1	Lysophospholipid s & Sphingolipids
LPS22.6	568.1	153.05	4.1	NA	LPS 17:1	Lysophospholipid s & Sphingolipids

Note: NA means nothing found.

Table S5. Detected polar metabolites in mouse muscle samples.

Metabolites name	ChEBI ID	Molar mass (M/Z)	Retention time (min)	ISTD	Class
<i>Analyzed by HILIC-MS method (negative ionization mode)</i>					
6-phosphogluconic acid	48928	275.0174	10.1	Fumarate-d ₂	Energy metabolites
Acetyl-CoA	15351	808.1185	7.4	Fumarate-d ₂	Energy metabolites
Adenosine	16335	266.0889	3.8	Pyruvate- ¹³ C ₃	Energy metabolites
ADP	16761	426.0221	9.4	AMP- ¹³ C ₁₀ , ¹⁵ N ₅	Energy metabolites
AMP	16027	346.0558	7.0	AMP- ¹³ C ₁₀ , ¹⁵ N ₅	Energy metabolites
Ascorbic acid	29073	175.0242	6.7	Valine- ¹³ C ₅	Energy metabolites
ATP	15422	505.9885	11.5	ATP- ¹³ C ₁₀ , ¹⁵ N ₅	Energy metabolites
cAMP	17489	328.0452	5.7	UMP- ¹⁵ N ₂	Energy metabolites
CDP	17239	402.0109	10.7	UMP- ¹⁵ N ₂	Energy metabolites
cis-Aconitate	16383	173.0085	6.7	Valine- ¹³ C ₅	Energy metabolites
CMP	17361	322.0446	8.8	UMP- ¹⁵ N ₂	Energy metabolites
CTP	17677	481.9772	13.0	UMP- ¹⁵ N ₂	Energy metabolites
Cytidine	17562	242.0776	5.7	Leucine-d ₃	Energy metabolites
Dihydroxyacetone-P	16108	168.9907	9.1	Fumarate-d ₂	Energy metabolites
Fructose-6-P	78697	259.0224	9.6	Fumarate-d ₂	Energy metabolites
GABA	16865	102.0561	10.6	Asparagine- ¹³ C ₄ , ¹⁵ N ₂	Amino acid
GDP	17552	442.0171	13.3	UMP- ¹⁵ N ₂	Energy metabolites
Glucose	17234	179.0561	7.5	Fumarate-d ₂	Energy metabolites
Glucose-1-P	58601	259.0224	9.1	Fumarate-d ₂	Energy metabolites
Glucose-6-P	14314	259.0224	10.2	Fumarate-d ₂	Energy metabolites
Glyceraldehyde-3-P	17138	168.9907	8.4	Fumarate-d ₂	Energy metabolites
Glycerate-3-P	58272	184.9857	9.2	Fumarate-d ₂	Energy metabolites
GMP	NA	362.0507	8.9	UMP- ¹⁵ N ₂	Energy metabolites
GTP	15996	521.9834	13.6	UMP- ¹⁵ N ₂	Energy metabolites
Guanosine	16750	282.0838	6.1	Isoleucine- ¹³ C, ¹⁵ N	Energy metabolites
Hypoxanthine	17368	135.0306	4.1	Pyruvate- ¹³ C ₃	Energy metabolites
IMP	17202	347.0398	7.9	UMP- ¹⁵ N ₂	Energy metabolites
Inosine	17596	267.0728	5.4	Leucine-d ₃	Energy metabolites
Malate	25115	133.0142	7.1	Fumarate-d ₂	Energy metabolites
Oxiglutathione	167606	611.1441	11.8	Asparagine- ¹³ C ₄ , ¹⁵ N ₂	Energy metabolites
Phosphoenolpyruvate	18021	166.9751	8.9	Asparagine- ¹³ C ₄ , ¹⁵ N ₂	Energy metabolites
Pyruvate	15361	87.0088	3.7	Pyruvate- ¹³ C ₃	Energy metabolites
Succinic acid	15741	117.0193	5.8	Succinate-d ₄	Energy metabolites

Simultaneous extraction of non-polar and polar metabolites

UDP	17659	402.9949	9.6	UMP- ¹⁵ N ₂	Energy metabolites
UMP	28895	323.0286	7.2	UMP- ¹⁵ N ₂	Energy metabolites
Uridine	16704	243.0616	4.3	Pyruvate- ¹³ C ₃	Energy metabolites
UTP	15713	482.9613	11.6	UTP- ¹³ C ₉ , ¹⁵ N ₂	Energy metabolites
Xanthine	15318	151.0255	3.9	Pyruvate- ¹³ C ₃	Energy metabolites
α -Ketoglutarate	80619	145.0142	6.7	Fumarate-d ₂	Energy metabolites
Tyrosine	18186	180.0666	7.4	Valine- ¹³ C ₅	Amino acid
Alanine	15570	90.0550	8.9	Glutamate- ¹³ C ₅ , d ₅ , ¹⁵ N	Amino acid
Phenylalanine	28044	164.0717	5.6	Leucine-d ₃	Amino acid
Asparagine	17196	131.0462	9.8	Asparagine- ¹³ C ₄ , ¹⁵ N ₂	Amine
Leucine	25017	130.0874	5.8	Leucine-d ₃	Amino acid
Ornithine	18257	131.0826	10.5	Asparagine- ¹³ C ₄ , ¹⁵ N ₂	Amino acid
<i>Analyzed by CE-MS method (positive ionization mode)</i>					
Creatine	16919	132.0768	9.6	Glycine-d ₂	Energy metabolites
Arginine	29016	175.1190	7.6	Valine- ¹³ C ₅	Amino acid
Spermidine	16610	146.1652	4.5	Glutamine- ¹³ C ₅	Amine
Aspartic acid	17364	134.0448	14.1	Aspartate- ¹³ C ₄ , d ₃ , ¹⁵ N	Amino acid
Lysine	18019	147.1190	7.2	Valine- ¹³ C ₅	Amino acid
Valine	27266	118.0863	11.4	Valine- ¹³ C ₅	Amino acid
Methionine	16811	150.0583	12.8	Isoleucine- ¹³ C, ¹⁵ N	Amino acid
Glutamine	28300	147.0764	12.7	Glutamine- ¹³ C ₅	Amine
Serine	17822	106.0499	11.8	Aspartate- ¹³ C ₄ , d ₃ , ¹⁵ N	Amino acid
Threonine	16857	120.0655	12.3	Aspartate- ¹³ C ₄ , d ₃ , ¹⁵ N	Amino acid
Glutamic acid	18237	148.0604	12.8	Glutamate- ¹³ C ₅ , d ₅ , ¹⁵ N	Amino acid
Glycine	15428	76.0393	9.8	Glycine-d ₂	Amino acid
Histidine	27570	156.0768	7.7	Valine- ¹³ C ₅	Amino acid
Tryptophan	16828	205.0972	12.5	Tryptophan- ¹³ C ₁₁ , ¹⁵ N ₂	Amino acid
4-Hydroxyproline	20392	132.0655	9.3	Valine- ¹³ C ₅	Amino acid
Proline	26271	116.0706	13.3	Valine- ¹³ C ₅	Amino acid
Creatinine	16737	114.0662	6.8	Glycine-d ₂	Amine

Note: NA means nothing found.